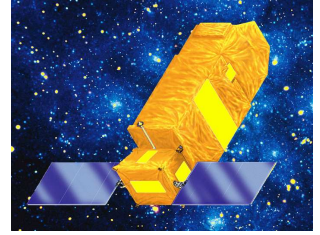
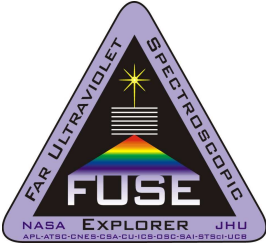


# Modeling FUSE Spectra of Cool Luminous Stars

A. Lobel & A. K. Dupree  
Smithsonian Astrophysical Observatory, MA

alobel@cfa.harvard.edu, adupree@cfa.harvard.edu



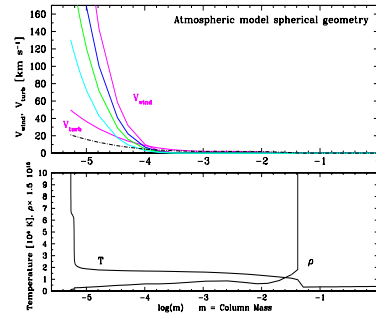
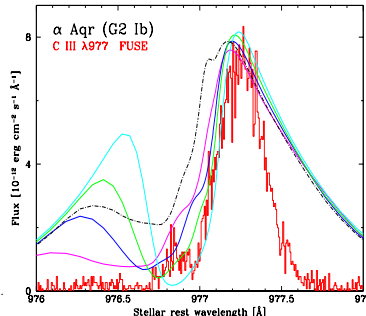
## Summary

We present a semi-empirical model for the thermodynamic and dynamic conditions of the chromosphere, and the lower transition region, of the hybrid supergiant  $\alpha$  Aqr (G2 Ib). Our modeling method is based on detailed dynamic non-LTE radiative transport calculations in spherical wind geometry. We find that the asymmetric profile of the C III  $\lambda 977$  resonance emission line, observed with *FUSE*, can be modeled with a supersonic outward accelerating wind structure. The line profile modeling reveals that the hot chromospheric, and lower transition region plasma is highly turbulent, with supersonic velocities, on small length scales in this luminous G-type star. This advanced modeling work is performed in conjunction with high-resolution near-UV spectra, obtained with *HST-STIS* for another early G-type Ib supergiant  $\beta$  Aqr, and for the late G-type supergiant  $\epsilon$  Gem (G8 Ib). The spectra serve to first develop reliable chromospheric models from detailed fits to the Mg II resonance lines, together with the H $\alpha$  profile from high-resolution ground-based observations. The chromospheric models are then built out into the lower transition region to model the *FUSE* spectra. We observe that the C III resonance profile of  $\alpha$  Aqr assumes a remarkable asymmetric shape, reminiscent of P Cygni profiles observed in hot luminous supergiants. The model indicates outflow velocities above  $\sim 140 \text{ km s}^{-1}$  at kinetic temperatures of 65,000 K and higher. A comparison of emission line morphologies observed with *FUSE* in  $\alpha$  Aqr and  $\beta$  Dra (G2 Ib-II), with *HST-STIS/GHRS* and *IUE* spectra is also presented.

This work is based on data obtained for the Guaranteed Time Team by the NASA-CNES-CSA *FUSE* mission operated by the Johns Hopkins University, and with the NASA/ESA *HST*, collected at STScI, operated by AURA Inc., under contract NAS5-26555. Financial support has been provided by NASA contract NAS5-32985, and by STScI grant GO-08280 to the Smithsonian Astrophysical Observatory.

## 1. FUSE, STIS, & Optical Spectra

*FUSE* spectra of the hybrid G2-type supergiant  $\alpha$  Aqr, and the less luminous G2 supergiant  $\beta$  Dra have been obtained for PI Science Team programs P118 and P218: *FUV Spectroscopic Survey of Cool Stars*. We present a comparative study of the transition region wind dynamics of  $\alpha$  Aqr with other cool luminous stars, to develop radiative transfer models of the thermal structure of the chromosphere and the lower transition region, and to determine their velocity and electron density structures. The C III  $\lambda 977$ , O VI  $\lambda 1031$  &  $\lambda 1037$  emission lines were observed on June 16 2001 for a total exposure time of  $\sim 34,400$  s. These lines were observed in  $\beta$  Dra on June 30 2001, with a total exposure time of  $\sim 16,400$  s. The presented line profiles have been calibrated with CalFUSE 2.0.5, and the separate exposures cross-correlated. High-resolution *STIS* near-UV spectra of  $\beta$  Aqr, also shown below for H Ly $\alpha$  and Mg II h & k, were obtained in a survey of late-type stars, including the G8 Ib-supergiant  $\epsilon$  Gem (G0 2880). High-resolution optical spectra of  $\alpha$  Aqr,  $\beta$  Dra,  $\beta$  Aqr, 9 Peg, and  $\epsilon$  Gem have been obtained with the UES and Sofis spectrographs (ING, La Palma) to complement this modeling work.



## 2. Non-LTE Atmospheric Modeling

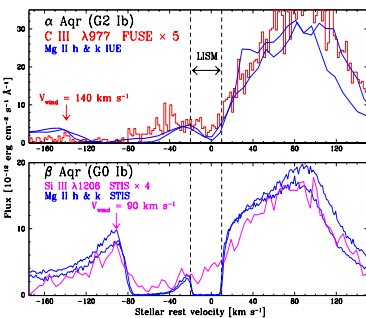
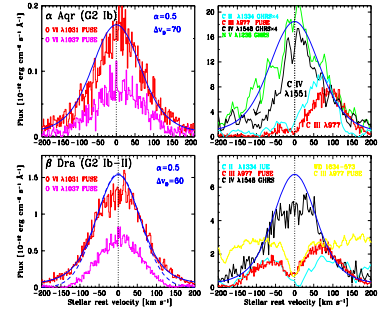
The left-hand figures show NLTE radiative transfer fits to C III  $\lambda 977$  through a semi-empirical model of the chromosphere and lower transition region (TR) of  $\alpha$  Aqr. The atmospheric model is shown in the column mass scale, with a rapid increase of  $T$  at  $\log(m) < -5.2$ . The outward decrease of  $\rho$  (or  $N_e$ ) produces a central scattering core in the computed emission profile, which assumes an asymmetric shape due to opacity in a fast accelerating wind. Best multi-level fits to the observed profile are obtained for  $V_{\text{wind}} > 140 \text{ km s}^{-1}$  in the lower TR ( $T \approx 65,000 \text{ K}$ ), which strongly scatters the blue emission line wing (magenta lines). The model signals a supersonic optically thick warm wind in the outer atmosphere of this supergiant with  $R_{\text{phot}} \approx 100 R_{\odot}$ ,  $T_{\text{eff}} = 5250 \text{ K}$  and  $\log(g) = 1.0$  are determined from best fits to high-resolution optical spectra with Kurucz models. Our chromosphere and TR model extends over  $10.4 R_{\text{phot}}$ . Supersonic increasing microturbulence velocities ( $V_{\text{turb}}$ ) are required in the upper chromosphere to fit the depth of the self-reversal in C III, and also its width in Ly $\alpha$  and Mg II for  $\beta$  Aqr (see 5).

## 3. C III P Cygni-type Line Profiles

The left-hand figure compares the detailed line shapes of the C III resonance line observed with *FUSE* (red), with the shapes of the *IUE* Mg II h & k resonance lines (blue). The overall C III line profile reveals a remarkable resemblance to the shape of the Mg II lines. At a distance of  $\sim 200$  pc  $\alpha$  Aqr has considerable extinction by the Local Interstellar Medium (LISM), which causes an absorption dip around the stellar rest velocity (dashed lines). Similar intensity saturated LISM absorption is observed in Mg II with *STIS* in another hybrid supergiant  $\beta$  Aqr at comparable distance ( $d \approx 188$  pc). The profiles in the lower panel are shaped due to the higher *STIS* resolution. The line profiles in both early G-type supergiants assume a remarkable asymmetric shape that resembles the P Cygni profiles observed in UV resonance lines of hot luminous stars. We observe in  $\alpha$  Aqr a weak but significant 'hump' in the C III profile at  $\sim 140 \text{ km s}^{-1}$ , that coincides with similar weak emission in the Mg II profiles. The intensity of the feature appears stronger in  $\beta$  Aqr around  $\sim 90 \text{ km s}^{-1}$ , due to a slower accelerating warm wind in Si III  $\lambda 1206$  (magenta) and Mg II, we model in 5.

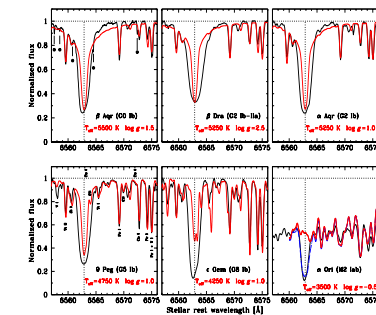
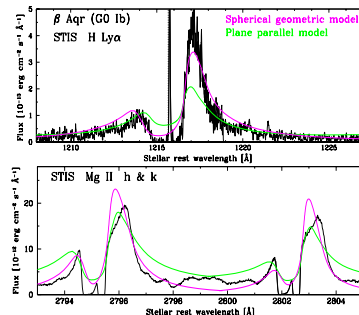
## 4. alpha Aqr (G2 Ib) vs. beta Dra (G2 Ib-II)

The O VI  $\lambda 1031$  &  $\lambda 1037$  resonance emission lines observed with *FUSE* in the right-hand figure (upper panels  $\alpha$  Aqr; lower  $\beta$  Dra) are more symmetric than C III  $\lambda 977$  (red), but show comparable line base widths in  $\beta$  Dra. The O VI lines form at higher kinetic temperatures (200–300 kK), and signal smaller opacity in a warm expanding wind of the upper transition region. For both stars we observe a striking resemblance between the overall line shapes of O VI and C IV  $\lambda 1551$  (black *GHRS*), and between the C III and C II  $\lambda 1334$  line profiles (cyan *IUE*). The C IV line assumes a P Cygni-type profile in  $\alpha$  Aqr (at arrow), while a more symmetric 'flat-topped' shape is observed in  $\beta$  Dra. This signals smaller transition region wind opacity for high ions in  $\beta$  Dra. The opacity in the warm wind decreases toward higher gravity stars, due to the smaller geometric extension of the line scattering region. Emission lines of intrinsically lower intensity are more symmetric due to the smaller scattering wind opacity. Note the contribution of LISM absorption (yellow) in C III of  $\beta$  Dra. The line appears however intrinsically asymmetric. Best fits to the emission line wings of high ions are obtained with Voigt profiles (blue), instead of a Gaussian (dashed).



## 5. Modeling Mg II, H Ly $\alpha$ , and H $\alpha$

The right-hand figures show best fits to high-resolution *STIS* spectra of H Ly $\alpha$  and Mg II in  $\beta$  Aqr. The fits are obtained for a detailed model of the photosphere, chromosphere, and lower transition region ( $T \leq 120 \text{ kK}$ ), similar to the model which fits C III in  $\alpha$  Aqr. The model is well constrained with radiative transport calculations in spherical geometry (magenta), and matches the depth of the central scattering core and the line wings. Plane parallel models do not fit the central core depth and overestimate the line wings. The wind model reproduces the observed component asymmetry and the  $u$ -shape of the central core. Note how a plane-parallel model reproduces the slanted shapes of the red Mg II emission components (green). Optical spectra of these G-type supergiants show how the photospheric contribution to H $\alpha$  (red) decreases toward later subclasses. The photospheric conditions obtained from our spectrum fits are indicated. In Betelgeuse (M2 Iab) the H $\alpha$  absorption is entirely of chromospheric origin (blue).



## Conclusions

- The asymmetric C III  $\lambda 977$  line observed with *FUSE* in  $\alpha$  Aqr can be modeled with radiative transfer through a fast accelerating transition region wind model.
- The thermal model requires a steep temperature increase from the upper chromosphere into the lower transition region.
- Supersonic outflow velocities are required to match the observed C III asymmetry.
- Supersonic microturbulence velocities are required to fit the depth and shape of the C III central scattering core, also observed in  $\beta$  Aqr for H Ly $\alpha$  and Mg II.
- C III  $\lambda 977$  and Mg II h & k assume P Cygni-type line shapes, also observed with *STIS* in  $\beta$  Aqr for Si III  $\lambda 1206$  and Mg II.
- O VI emission with *FUSE* in  $\alpha$  Aqr and  $\beta$  Dra signal smaller scattering opacity in an expanding hot transition region wind.